GSI

GSI-Preprint-97-08
Januar 1997

FRAGMENTATION OF 270 A MeV CARBON IONS IN WATER
M. Golovkov, D. Aleksandrow, L. Chulkov, G. Kraus, D. Schardt

A DETECTION SYSTEM FOR THE VERIFICATION OF 3D DOSE DISTRIBUTION
C. Brusasco, D. Schardt, B. Voss

THERAPY PLANNING FOR HEAVY ION IRRADIATION
M. Krämer, O. Jäckel

(Presented at the 'Second Int. Symposium on Hadron Therapy', Switzerland,Sept 9-13,1996)

Gesellschaft für Schwerionenforschung mbH
Planckstraße 1 • D-64291 Darmstadt • Germany
Postfach 11 05 52 • D-64220 Darmstadt • Germany

Contribution to Second Int. Symposium on Hadrontherapy, Switzerland, 9-13 Sept. 1996

Fragmentation of 270 A MeV carbon ions in water

M. Golovkov[1], D. Aleksandrov[1], L. Chulkov[1], G. Kraus[2] and D. Schardt[2]
[1] *Kurchatov Institute Moscow, Russia*
[2] *Biophysik, Gesellschaft für Schwerionenforschung, Darmstadt, Germany*

Introduction

In heavy-particle therapy the effect of nuclear fragmentation may cause a significant alteration of the radiation field. Nuclear collisions occuring along the penetration path of high-energy ions in tissue cause a loss of primary beam particles and the build-up of lower-Z projectile fragments. As a consequence, the dose distribution along the beam path is different as compared to the dose profile which would result from the passage of primary ions in absence of nuclear reactions. In particular, the lower-Z fragments which have longer ranges than the primary particles cause an additional dose contribution beyond the Bragg peak. Furthermore, the biological efficiency of the reaction products is different from the primary ions and has to be included in the calculation of the biological effects, especially for the target volume. The importance of these effects generally increases as a function of the beam energy (or penetration depth). For a ^{12}C beam of 200 A MeV, for example, about 30 % of the primary particles undergo nuclear reactions and do not reach the Bragg maximum at 8.5 cm depth in water. The physical models used in therapy planning codes have to take into account these effects and therefore require detailed knowledge of the fragmentation processes in tissue.

Fragmentation reactions have been extensively studied for many years [1, 2]. The general features of projectile fragmentation are well described on the basis of the Goldhaber model [3]. The first experimental fragmentation study of relativistic ^{12}C and ^{16}O beams was performed by Greiner et al. [4]. It was found that the projectile fragments have a velocity close to that of the beam particles and their momentum distributions in the projectile rest frame are typically Gaussian shaped, except for hydrogen fragments which showed an additional exponential component.

In previous experiments [5] at GSI the fragmentation characteristics of various light ion beams in the energy range between 200 and 670 A MeV using water as a tissue-equivalent material was investigated. Elemental yields for projectile fragments down to Z=5 and total and partial charge-changing reaction cross sections were obtained. In continuation of these studies we present here an analysis of longitudinal and transverse momentum distributions of projectile fragments which were produced by a primary ^{12}C beam in thick water absorbers. The experimental set-up was designed for the detection of low-Z fragments including helium and hydrogen.

Experimental set-up

The arrangement of beam detectors, water absorber, and fragment detectors is shown in Fig.1. The 270 A MeV ^{12}C beam delivered by the heavy-ion synchrotron SIS passed through a thin

Address for correspondence: Dieter Schardt, Biophysik, Gesellschaft für Schwerionenforschung, Planckstr.1, D-64291 Darmstadt, Germany

vacuum exit window (0.1 mm steel) and a beam counter (plastic scintillator 1.5 mm thick) which gave the start signal for time-of-flight (TOF) measurements. A multiwire proportional chamber (MWPC) was used for beam alignment. The water absorber consisted of one or two thin-walled plastic bottles, corresponding to 4.26 or 8.52 g/cm^2 of water. This means about 0.17 or 0.34 interaction lengths for the primary carbon beam. The projectile fragments were detected in two large scintillator arrays [6] which are parts of the TOF-wall of the ALADIN spectrometer [6] at GSI and were available for these measurements. They were placed about 3.4 m downstream, covering forward emission angles from 3° to 19° (array 1) and from 26° to 43° (array 2) in the laboratory frame. These detectors gave information on the fragments nuclear charge Z_f (via energy loss signal ΔE), the emission angle (detected position), and the fragment velocity (TOF). Each scintillator array consisted of eight plastic scintillator paddles of 5 mm thickness and an active area of 1000x40 mm^2. Each paddle was coupled to photo multiplier tubes at both ends. From the time differences of the two signals the position of the hit along one paddle was deduced.

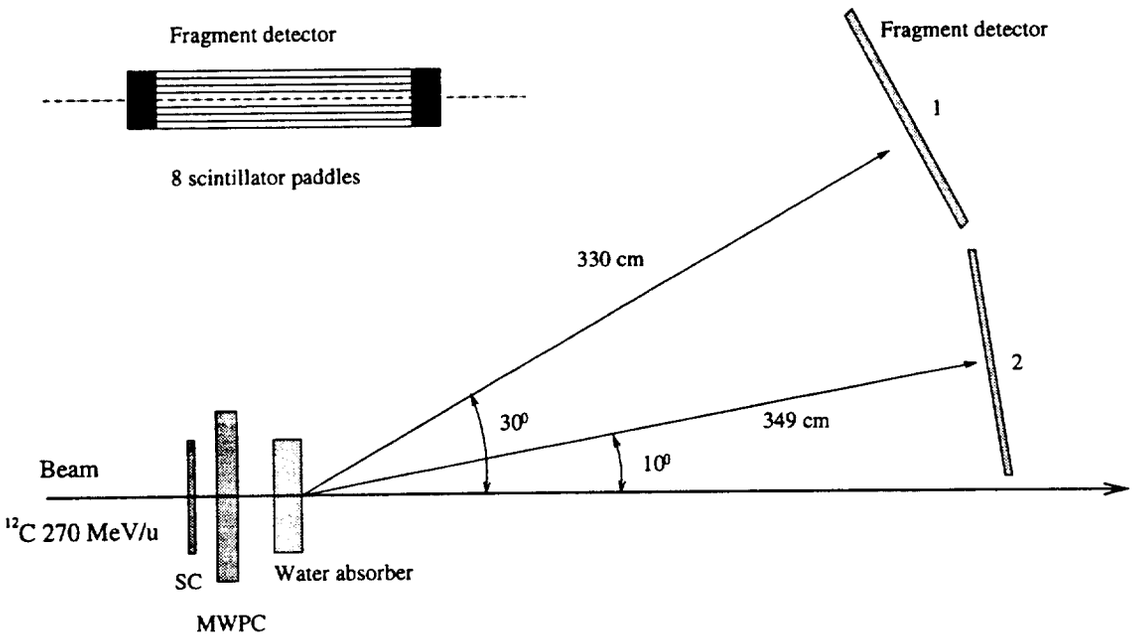

Fig.1: Experimental set-up used for fragmentation measurements. Passing through a scintillation counter (SC) and a multiwire chamber (MWPC), the ^{12}C beam hit a thick water absorber. The emerging projectile fragments were detected in two large position-sensitive scintillator arrays. The velocities of the fragments were obtained from time-of-flight measurements.

The time resolution of these detectors was about 150 ps and varied by about 20% from paddle to paddle. The corresponding position resolution was 2-3 cm FWHM. For the position calibration, a shielding wall consisting of of lead bricks with 10 mm wide vertical air gaps was mounted in front of the TOF detectors. This wall was illuminated with protons and alpha particles with a broad angular distribution which were produced by stopping the carbon beam in a thick target.

An example of the fragment charge identification for Z=1,2 is shown in Fig.2. The time scale was obtained from a pulser calibration using a set of calibrated delay lines. The absolute time scale was deduced from the calculated beam velocity for the Z=6 beam particles detected

at the smallest angle. The energy loss of the beam particles in all materials traversed (vacuum window, detectors, target, air) were taken into account in the data analysis.

The energy thresholds of the TOF detectors were found at about 1.5 - 2 MeV for the registration of protons. A walk correction was not done but those paddles of the scintillator array which showed a large walk effect were excluded in the analysis of light fragments (Z=1,2) where this effect leads to a pronounced distortion.

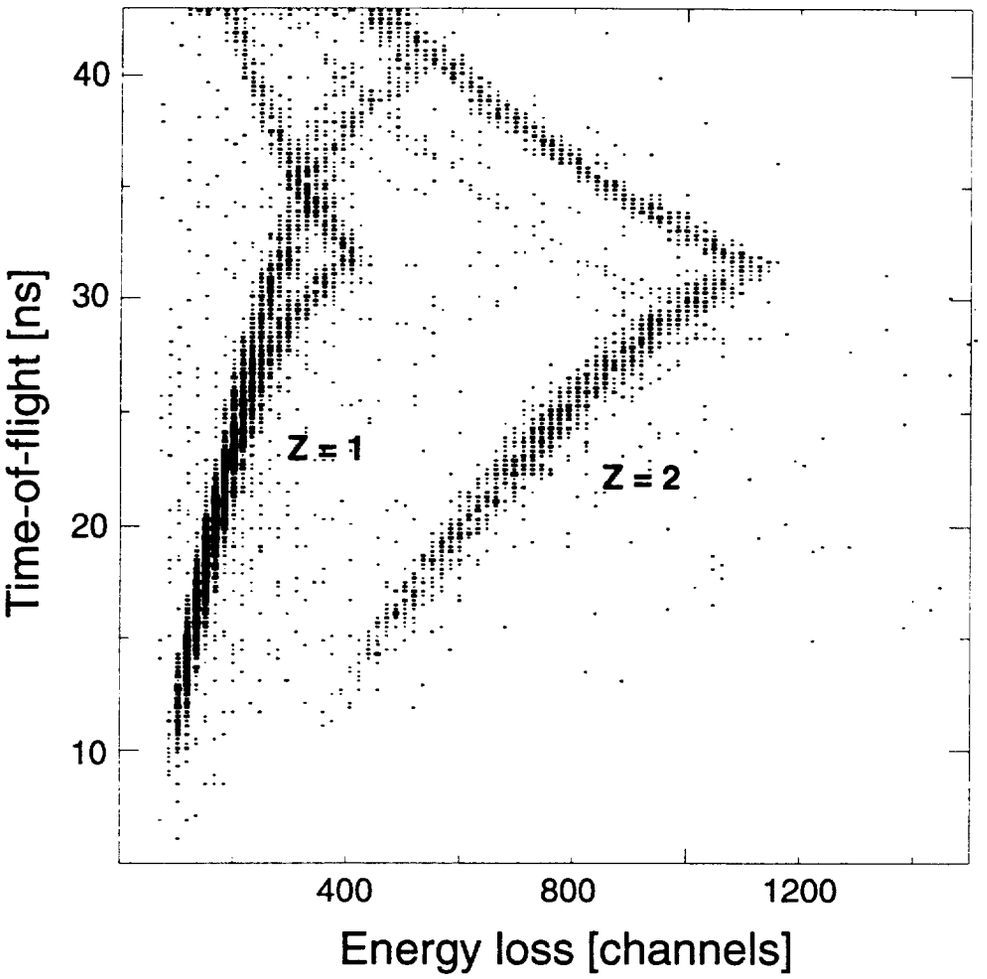

Fig.2: Scatterplot of time-of-flight versus energy loss ΔE measured with the scintillator arrays shown in Fig.1. The charges of the lightest nuclear fragments hydrogen and helium can be clearly separated. The point of change in slope corresponds to the case where the fragments do not have enough energy to pass through the scintillator and deposit their full energy. The splitting of the hydrogen branch is due to different isotopes (p,d,t). An indication of ^6He can be seen in the helium branch.

Results

Angular and momentum distributions

The position spectra which were measured with the scintillator arrays were transformed to angular distributions of the fragments in the laboratory frame. The effect of multiple scattering of fragments in the target material does not play a significant role for the absorber thicknesses

used here and was not taken into account.

The longitudinal momentum distributions of the fragments were obtained from the measured TOF-spectra and recalculated to the momenta at mid-position of the water absorber, applying corrections for energy losses in the water absorber and air. The nonlinearity of TOF due to the continuous energy losses of fragments in air between the water absorber and the TOF detector was taken into account by integrating backwards the velocity along the fragment's path. The momentum of the beam particles in the middle of the water absorber was calculated to be 705.7 A MeV/c (corresponding to an energy of ^{12}C 237.2 A MeV) for 4.26 g/cm^2 of water and 660.5 A MeV/c (210.4 A MeV) for 8.52 g/cm^2 of water. The overall TOF resolution of 0.5 ns FWHM corresponds to 17 A MeV/c in the momentum (velocity) scale and does not significantly affect the widths of the measured longitudinal momentum distributions.

Z=1 Fragments

The angular distribution of Z=1 fragments is shown in Fig 3 (left part). The Gaussian fit according to the Goldhaber model [3] underestimates the experimental data significantly. A Lorentz function overestimates the data at large angles. The best fit to the data is obtained by a pure exponential function $\sim exp(-\vartheta_{lab.}/\lambda)$ with parameter $\lambda = 5.3^0$. The deviation from the Gaussian shape for hydrogen fragments was first observed by Greiner et al. [4] in the analysis of fragmentation of relativistic ^{12}C and ^{16}O projectiles.

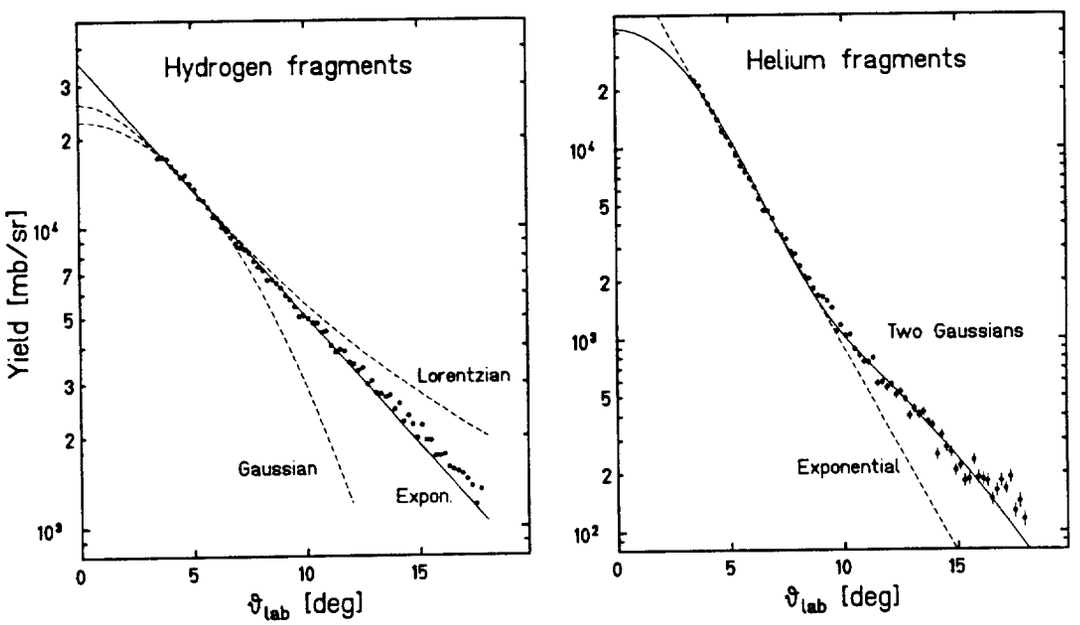

Fig.3: Angular distributions of hydrogen and helium fragments.

Longitudinal momentum distributions for fragments with Z=1 to Z=5 are presented in Fig.4. The shape for Z=1 fragments looks Gaussian with the mean value close to the beam velocity and some tail at the low momentum side. The Z=1 distributions were analyzed at different angles and fitted by the Gaussian function

$$F(p) = Cexp(-\frac{(p-p_0)^2}{2\sigma^2})$$

With increasing angle ($\vartheta_{lab} = 4^0$ to 15^0) the width σ changes from 63 to about 90 A MeV/c and the mean momentum decreases from 684 to 611 A MeV/c.

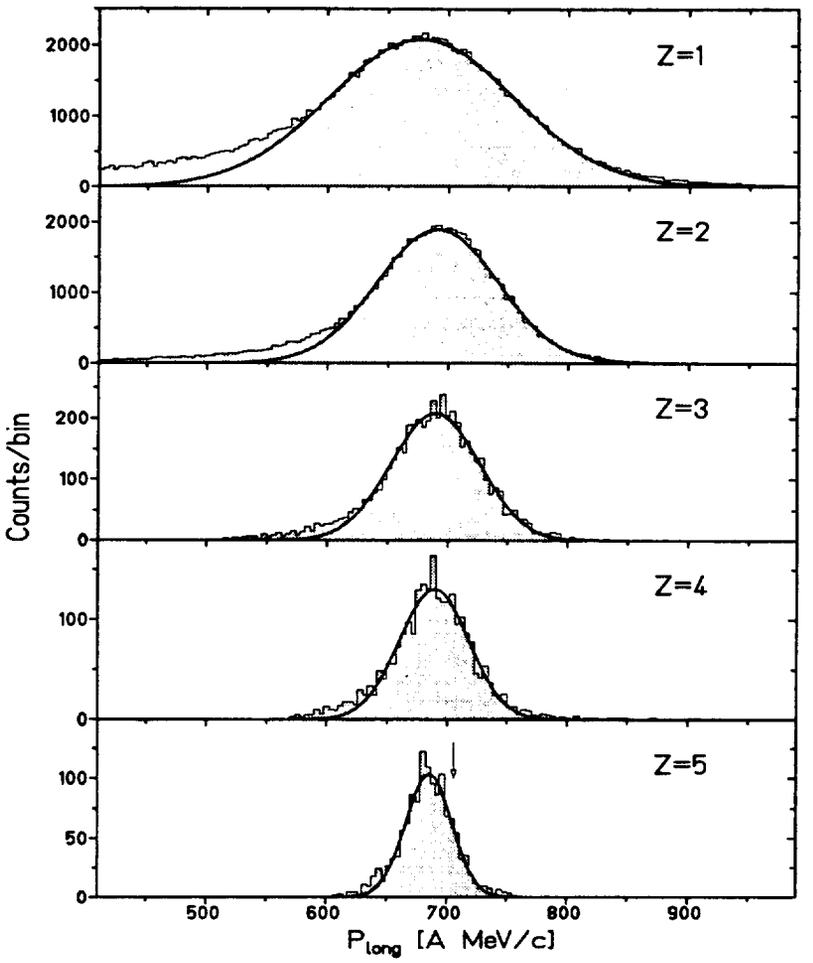

Fig.4: Comparison of longitudinal momentum distributions obtained from time-of-flight data for projectile fragments with nuclear charges Z=1 to Z=5. The arrow indicates the velocity of the primary ^{12}C ions.

Z=2 Fragments

The angular distribution of Z=2 fragments is shown in the right part of Fig.3. A change of the slope appears near $\vartheta_{lab} = 9^0$. Therefore at least two components are needed to fit the experimental data. The data were fitted by two Gaussians

$$F(p_\perp) = A_1 exp(-\frac{p_\perp^2}{2\sigma_{1\perp}^2}) + A_2 exp(-\frac{p_\perp^2}{2\sigma_{2\perp}^2})$$

where $p_\perp = p_o sin\vartheta_{lab}$ is the transverse momentum and $A_{1,2}$ and $\sigma_{1,2\perp}$ are free parameters. A similar fit was applied to describe the longitudinal momentum distributions of Z=2 fragments at different angles. For the fit of the longitudinal momentum the function

$$F(p) = P_1 exp(-\frac{(p-p_1)^2}{2\sigma_{1||}^2}) + P_2 exp(-\frac{(p-p_2)^2}{2\sigma_{2||}^2})$$

was used. In a first step all six parameters ($P_{1,2}$, $p_{1,2}$ and $\sigma_{1,2||}$) were free. After comparing these parameters at different angles we noted that the $\sigma_{||}$'s are almost independent of the angle and

$p_{1,2}$ follow a $cos\vartheta_{lab}$ law, i.e. $p_{1\|} = p_{10}cos\vartheta_{lab}$, $p_{2\|} = p_{20}cos\vartheta_{lab}$. In a second step it was possible to obtain a good fit of the momentum distributions at all measured angles, using the fixed parameters p_{10}=699, $\sigma_{1\perp}$=34.9, $\sigma_{1\|}$=45.5, p_{20}=605, $\sigma_{2\perp}$=67.9, $\sigma_{2\|}$=69.1 (all numbers in units of A MeV/c) and fitting only the two free parameters P_1 and P_2. The fixed parameters have uncertainties of about 10%. The widths of the parallel and transverse momentum distributions are equal within the uncertainty for the two components. The width of the first component is close to the prediction of the Goldhaber model of 38.4 A MeV/c with σ_o=90 MeV/c and its mean momentum is close to that of the beam (705 A MeV/c). It is obvious that such a decomposition of momentum distributions with two Gaussians is rather arbitrary. There is no justification for this by any model, but a similar picture has been observed for beryllium and boron isotopes in fragmentation of carbon beams on boron, carbon and silver targets [7]. There the appearance and development of the second component in the spectra at the largest laboratory angles (15° and more) was related with more central collisions.

Z=3,4,5 Fragments

The higher-Z fragments have rather narrow angular distributions and the yields for these isotopes at the minimum angle (3.5°) accessible in the experimental set-up shown in Fig.1 are below 10% of the maximum yield at zero degree. In order to cover the small angle region we have used the simple set-up sketched in the inset of Fig.5 and obtained angular distributions of carbon fragments by moving a single scintillation detector at a distance of 3,40 m from the water absorber perpendicular to the beam axis. The Z-identification of the fragments was done by the measured energy loss spectrum (Fig.5 right part), the angular distributions obtained from this measurement are shown in the left part of Fig.5, in logarithmic scale. At larger angles deviations from the Gaussian-like shape are observed.

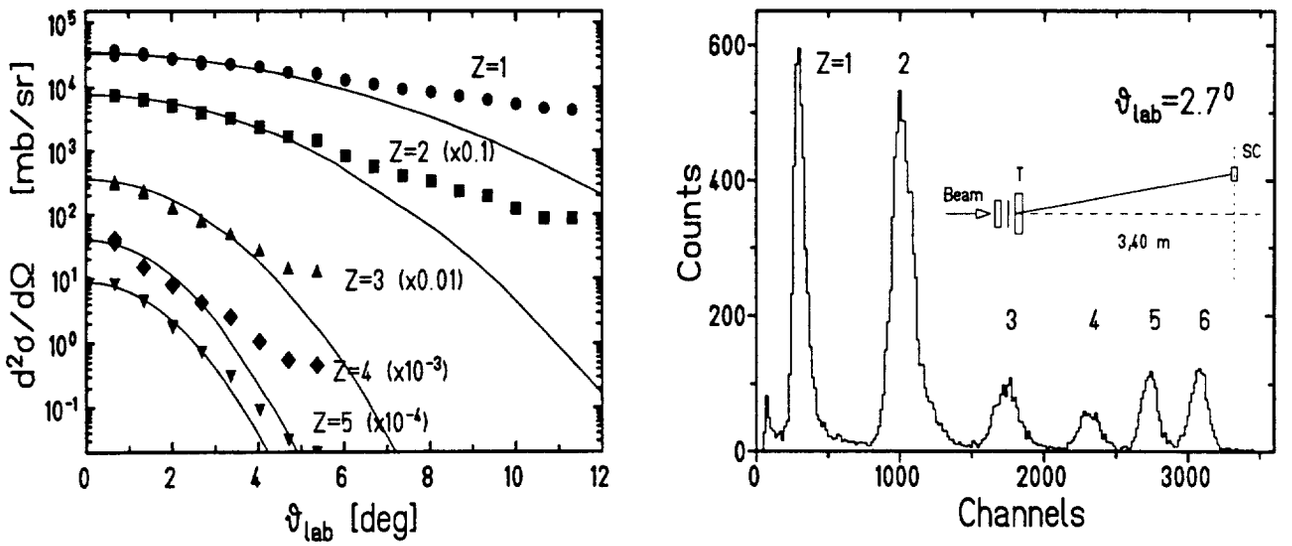

Fig.5: Differential yields of projectile fragments with nuclear charge Z=1 to Z=5 for the interaction of 270 A MeV ^{12}C ions on a water target (left). Energy loss spectrum obtained with a 9 mm thick plastic scintillator at an angle of 2.7° (right).

Elemental fragment yields

The elemental fragment yields, which we define as the number of fragments with a given element number produced in the absorber normalized to the number of incoming beam particles, are presented in Table 1. The main contributions to the uncertainties of about 10 % come from the account of dead time of the data acquisition system. The yields of Z = 1,2 fragments were obtained by integration of the fit functions which best reproduced the experimental angular distributions over all measured angles. The yields of Z = 3,4,5 were taken from the measurements shown in Fig.5 which were performed only for the 4.26 g/cm^2 water absorber.

Table 1: Elemental fragment yields for a 270 A MeV ^{12}C beam passing through water absorbers of 4.26 and 8.52 g/cm^2 thickness

Fragments	B	Be	Li	He	H
4.26 g/cm^2 water	0.0288(16)	0.0142(31)	0.0224(13)	0.123(11)	0.242(20)
8.52 g/cm^2 water	-	-	-	0.257(23)	0.460(45)

Summary

Nuclear fragmentation reactions may cause a significant alteration of the radiation field in tissue which has to be taken into account in the physical models used in therapy planning codes. Using 270 A MeV ^{12}C beams delivered by the heavy ion synchrotron SIS we studied the characteristics of light fragments produced in water absorbers of 4.26 and 8.52 g/cm2 thickness. Angular distributions and longitudinal momentum distributions were measured by means of a segmented scintillator wall covering emission angles of up to 40 degrees. The lighter fragments have a rather broad angular distribution and deviations of the momentum distributions from predictions of the Goldhaber model were observed. For hydrogen fragments the angular distribution shows an exponential behaviour, the longitudinal momentum distribution looks Gaussian with a low-momentum tail. For helium fragments we found that both transverse and longitudinal momentum distributions are well described in the rest frame of the projectile by the sum of two Gaussians. For both Gaussians the widths of the transverse and longitudinal momenta are equal within the error bars.

Acknowledgement

We wish to thank the ALADIN group at GSI for leaving us their scintillator arrays for these measurements.

References

[1] Goldhaber AS and Heckman HH, High energy interactions of nuclei, Ann. Rev. Nucl. Part. Sci. 1978; 28; 161-205.

[2] Friedlander EM and Heckman HH, Relativistic heavy-ion collisions: experiment, in: Treatise on heavy-ion science, Vol.4, Bromley DA (ed.), Plemum, New York, 1985; 403-562.

[3] Goldhaber AS, Statistical models of fragmentation processes, Phys. Lett. B 1974; 53; 306-308.

[4] Greiner DE, Lindstrom PJ, Heckman HH, Cork B, Bieser FS, Momentum distributions of isotopes produced by fragmentation of relativistic ^{12}C and ^{16}O projectiles, Phys. Rev. Lett. 1975; 35; 152-155.

[5] Schall I, Schardt D, Geissel H, Irnich H, Kankeleit E, Kraft G, Magel A, Mohar MF, Münzenberg G, Nickel F, Scheidenberger C, Schwab W, Charge-changing nuclear reactions of relativistic light-ion beams ($5 \leq Z \leq 10$) passing through thick absorbers, Nucl. Instr. and Meth. B 1996; 117; 221-234.

[6] Schüttauf A et al., Universality of spectator fragmentation at relativistic bombarding energies, Nucl. Phys. A 1996; 607; 457-486.

[7] Guet C, Nucl. Phys. A 1983; 400; 191c-220c.